Empirical Site Amplifications at the Strong Motion Stations in the Kansai Region

○Miroslav HALLO, Kimiyuki ASANO, Haruko SEKIGUCHI, Tomotaka IWATA

1. Introduction

The earthquake shaking observed on the Earth's surface is a result of source, path, and site effects. Site effects, such as site amplification, are caused by the wave propagation through the local soft-rock and sediment layers and can vary significantly over short lateral distances. The site amplification can be an origin of significant earthquake damage; hence, it should be precisely evaluated, especially in urban areas such as Osaka, Kyoto, and Nara basins in the Kansai region.

In this study, we evaluate empirical site-specific amplification functions in the spectral domain from earthquake data recorded by strong motion stations at 454 sites in the Kansai region. We developed and applied a spectral inversion method (e.g., Iwata and Irikura, 1986), considering also the high-frequency attenuation. It resulted in a database of empirical amplification functions in the freq. range 0.8–30 Hz.

2. Method

In our formulation of the spectral inversion approach, acceleration earthquake spectra $U(f)$ are expressed as

$$U(f) = (2\pi f)^2 \, M_0 \frac{F_{\theta\varphi} F_S F_R}{4\pi\rho V_S^3} \left(1 + \left(\frac{f}{f_c}\right)^2\right)^{-1} \times \frac{1}{d} \exp\left(\frac{-\pi f d}{V_S Q(f)}\right) \times |H(f)| \exp(-\pi f \kappa) \, G(f) \qquad (1)$$

in which f is frequency, M_0 is the scalar seismic moment, $F_{\theta\varphi}$ is the *S*-wave radiation pattern, F_S is the free surface effect coefficient, F_R is the radiation energy ratio, ρ and V_S are density and *S*-wave velocity of the bedrock, f_c is the source corner frequency, d is the distance, $Q(f)$ is the *S*-wave quality factor, $H(f)$ is surface-to-outcrop *SH*-wave transfer function of the reference velocity model, κ is high-frequency attenuation of the reference velocity model, and $G(f)$ is the site-specific amplification.

Inputs of our inversion approach are M_0, d, $F_{\theta\varphi}$; outputs are f_c (or the stress drop) and $G(f)$. Regional attenuation $Q(f)$ is from Petukhin *et al.* (2004), and the reference velocity model from Poggi *et al.* (2013). The inversion procedure consists of three steps:

- Invert for preliminary site amplifications using a constant stress drop of 1 MPa for all earthquakes,
- Invert for stress drops of all earthquakes using preliminary site amplification functions,
- Invert for final site amplification functions using earthquake-specific stress drops.

3. Data

We analyze 227 regional crustal earthquakes from the period 1997–2025 ($M_{\mathrm{JMA}} > 3$, $d < 120$ km, and depth < 35 km) recorded at 454 sites in the Kansai by:

- K-NET and KiK-net networks operated by the National Research Institute for Earth Science and Disaster Resilience (NIED, 2019a; Aoi *et al.*, 2020),
- Shindo-kei stations by the Japan Meteorological Agency (JMA) and local governments,
- strong-motion stations operated by the Committee of Earthquake Observation and Research in the Kansai Area (CEORKA),
- and stations operated by the Disaster Prevention Research Institute (DPRI) of Kyoto University.

Scalar seismic moments M_0 and *S*-wave radiation patterns $F_{\theta\varphi}$ are derived from moment tensors of the F-net catalogue (NIED, 2019b).

4. Results

The empirical site-specific amplification functions are evaluated separately for all horizontal components of recorded earthquakes, accounting for azimuthal dependence. As an example, in Fig. 1, see the empirical site-specific amplification for station FKS located in the Fukushima ward in Osaka. This site is characterized by a very deep sedimentary basin floor (bedrock depth > 1.5 km) and soft sediments due to its proximity to the mouth of the Yodo River. Our results show that it is characterized by strong amplification at the frequency range 0.13–2 Hz (i.e., period 0.5–7.7 s).

Based on the dense spatial coverage, we constructed regional maps of empirical amplification for periods of 5, 2, 1, 0.5, 0.2, and 0.1 s. Long-period amplification (period of 5 s) is pronounced only near the Yodo River mouth and in Higashiosaka City. Periods of 1–2 s are strongly amplified in the central areas of the Osaka and Nara basins, and in the southern Kyoto basin. In contrast, short periods of 0.1–0.2 s show significant amplification throughout various sites at the Nara and Kyoto basins, but not in the Osaka basin.

Next, we created a list of sites with empirical amplifications close to one (rock outcrop sites), which can be used as reference sites: DIG, HSD, KTR, HYG027, OSKH04, and WKYH09 (surface sensors).

Inferred earthquake stress drops have a median of 0.85 MPa which is consistent with Nakano *et al.* (2015).

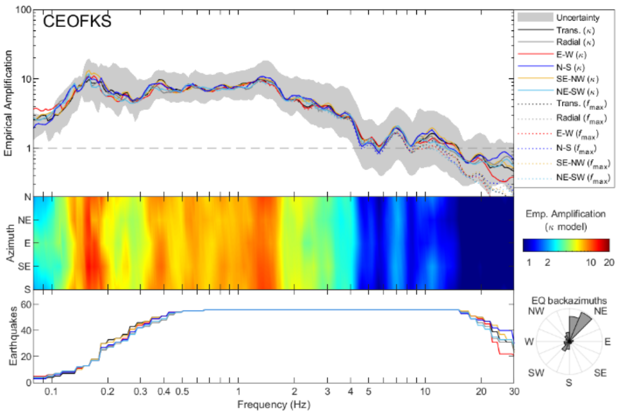

Figure 1. *Empirical site amplification function of the FKS strong-motion station (CEORKA network) located in the Fukushima ward in Osaka (i.e., deep basin site).*

5. Conclusions

We evaluated empirical site amplifications in the frequency range 0.8–30 Hz for 454 instrumented sites in the Kansai area and created regional empirical site-amplification maps. We find that the longest periods of the band with significant amplification correlate with bedrock depth, reaching up to 7.7 s determined for deep basin sites in Osaka. Moreover, the shapes of amplification functions are comparable to those of Tsurugi *et al.* (1997), which were evaluated at ten CEORKA sites in the Osaka basin.

Acknowledgments

The authors acknowledge the NIED, JMA, CEORKA, DPRI, and local governments for operating monitoring stations used in this study. M. Hallo was supported by the Japan Society for the Promotion of Science (JSPS) through fellowship number P23070, Grant-in-Aid 23KF0149, and the "Research Project for the Advancement of Long-term Evaluation Methods for Inland Earthquakes, Including Those Occurring on Active Faults" by the Ministry of Education, Culture, Sports, Science and Technology (MEXT).

References

Aoi S, Asano Y, Kunugi T, *et al.* (2020). MOWLAS: NIED observation network for earthquake, tsunami and volcano, *Earth Planets Space* **72**:126.

Iwata T and Irikura K (1986). Separation of source, propagation and site effects from observed S-waves, *J Seismol Soc Jpn* **39**, 579–593.

Nakano K, Matsushima S, Kawase H (2015). Statistical properties of strong ground motions from the generalized spectral inversion of data observed by K-NET, KiK-net, and the JMA Shindokei network in Japan, *Bull Seismol Soc Am* **105**, 2662–2680.

NIED (2019a). NIED K-NET, KiK-net, National Research Institute for Earth Science and Disaster Resilience. DOI: [10.17598/NIED.0004](https://doi.org/10.17598/NIED.0004)

NIED (2019b). NIED F-net, National Research Institute for Earth Science and Disaster Resilience. DOI: [10.17598/NIED.0005](https://doi.org/10.17598/NIED.0005)

Petukhin A, Irikura K, Kagawa T, Ohmi S (2004). Study of the seismic attenuation in Kinki region, Japan, using the ray theory elastic attenuation effect in 3-D velocity model and the 3-D structure of Q-value, *13 WCEE*, paper 633, Vancouver, Canada.

Poggi V, Edwards B, Fäh D (2013). Reference S-wave velocity profile and attenuation models for ground-motion prediction equations: Application to Japan, *Bull Seismol Soc Am* **103**(5), 2645–2656.

Tsurugi M, Tai M, Irikura K, Kowada A (1997). Estimation of empirical site amplification effects using observed records, *J Seismol Soc Jpn* **50**, 215–227.